

Experimental study on a long-time working solid-fuel scramjet combustor

Guanlin Fang*, Zhijun Wei*, Zhiwen Wu*†, Changchao Guo**, Lihe Wang*, Rui Du*, Hao Zhang*, and Ningfei Wang*

*Beijing Institute of Technology (BIT), 5 South Zhongguancun Street, Haidian District, Beijing, 100081, CHINA
Phone: +86-010-6891-3623

† Corresponding author: bitwzw@bit.edu.cn

**Xi'an Modern Chemistry Research Institute, 168 East Zhangba Road, Yanta District, Xi'an, 710065, CHINA

Received: November 19, 2017 Accepted: October 12, 2018

Abstract

The characteristics of a long-time working solid-fuel scramjet combustor have been investigated by experiments and theoretical calculation. Poly-methyl-methacrylate (PMMA) was used as solid fuel and a methane vitiated air heater was designed and built to simulate the flight environment of Mach 6 at a 25 km altitude, where the corresponding inlet total temperature and total pressure was 1600 K and 2.4 MPa. Flow and combustion phenomena were studied by recording combustor pressure and combustion video. The combustion process was analyzed, the fuel regression rate, specific thrust and specific impulse decrease gradually with time, the fuel mass flow rate remains constant. Comparing combustors with cavity or step, the characteristics of self-ignition and self-sustained combustion were studied, which were not consistent with the results from previous works. The results show that with enough inlet total temperature, even with step, self-ignition can also succeed, but it cannot maintain stable combustion, until a cavity appeared in combustor.

Keywords: pmma, experiment, scramjet, self-ignition

Nomenclature

A	= area
L	= length of combustor
d	= diameter
x	= axial distance
F	= thrust
m	= mass flow rate
Ma	= Mach number
p	= pressure
r	= fuel regression rate
t	= combustor working time
T	= initial temperature of solid fuel
v	= velocity
k	= ratio of specific heat

Greek

ρ	= density
α	= half expanding angle

Subscripts

a	= ground atmospheric environment
e	= at the exit of combustor

cyl	= constant diameter cylindrical section
fh	= flameholding zone
flight	= flight environment parameters
ground	= ground test condition
ideal	= ideal condition
in	= combustor inlet
s	= solid phase
sp	= specific
0	= total parameter

1. Introduction

Studies have found that when the flight Mach number exceeds 5, airflow in the combustor burning in a supersonic flow can obtain a greater specific impulse and reduce the total pressure loss. So, supersonic combustion ramjet (scramjet) receives a great deal of attention.

At present, almost all scramjets have focused on liquid fuel, there are few solid-fueled scramjet research. Solid-fuel scramjet is a ramjet that pours or glues the solid fuel into the combustor to make a direct combustion with the

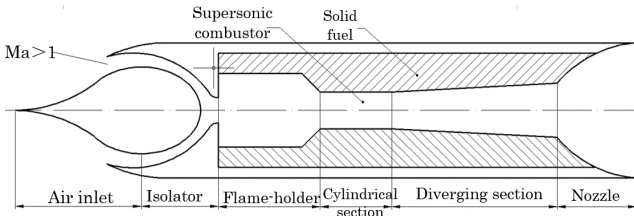


Figure 1 Configuration of the solid fuel scramjet.

supersonic flow. It has the advantages of a simple structure, responsive, easy storage and transportation. As shown in Figure 1, it consists of inlet, combustor and nozzle.

Hypersonic flow ($Ma > 5$) is compressed into a low Mach number supersonic flow through the air inlet and isolator, while the temperature and pressure increase. The high-temperature, high-pressure, high-speed airflow reacts with solid fuel near the wall in the combustor which melts, decomposes and burns. The chemical energy of the fuel is transformed into intrinsic energy of airflow. Through the nozzle, the pressure and temperature decrease, the Mach number increases. The intrinsic energy of airflow is transformed into kinetic energy to promote the aircraft flight.

From 1989 to 1991, Witt¹⁾ and Angus^{2),3)} in the Naval Postgraduate School made an initial study on the concept of the solid fuel scramjet. In their experimental research, the combustors were designed with the polymethyl methacrylate (PMMA) and the hydroxyl-terminated polybutadiene (HTPB), they added a bit of hydrogen into the combustor as the pilot torch to aid ignition and flame holding. In 1994–1998, a series of experimental studies were made by Ben-Yakar⁴⁾ and Gany⁵⁾ in the Israel Institute of Technology. These studies proved that solid fuel (PMMA) could self-ignite at the inlet parameters of total temperature 1200 K, total pressure 16 atm, Mach number 1.6. And they analyzed the effects of combustor configuration on the ignition and average fuel regression rate. Cohen⁶⁾ and Natan carried out further research to improve inlet total temperature, total pressure and mass flow rate, extended the application of the solid fuel scramjet. Saraf⁷⁾ studied the effects of metalized and non-metalized solid fuel by experiment. The results showed that the regression rate of metalized fuel was slightly larger than non-metalized fuel. Simone^{8),9)} conducted a numerical investigation using LiH as the solid fuel. The results showed that LiH is a good candidate for scramjet applications with high-energy density and safety. Huan Tao¹⁰⁾, Hong-wei Chi¹¹⁾, Chang-xiu Liu¹²⁾ and Biao Li¹³⁾, from Beijing Institute of Technology, made numerical studies on the self-ignition, stable combustion, flow field characteristics and combustion in non-designed conditions (Mach 4–6). Pei^{14),15)} investigated the combustion process and the performance change during the regression of solid fuel in SFSCRJ numerically. The results demonstrated that the degree of fuel diffusion increases and the combustion efficiency increases globally as the combustion process. Wang^{16),17)} simplified the calculation of unsteady combustion and flow in the solid fuel scramjet combustor

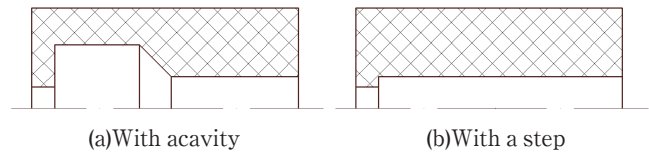


Figure 2 Cavity and step.

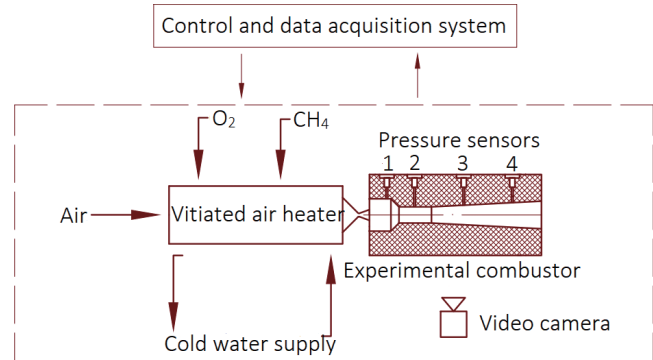


Figure 3 Schematic of the experimental system.

and presented a quasi-one-dimensional numerical method. They also discussed the specific thrust variation process and the reasons by the quasi-one-dimensional numerical method and experiment.

Many of the previous studies of scramjet mainly focused on a short time working combustor (less than 15 s) at a low total temperature (less than 1500 K). And there was a lack of studies on the operating characteristics of different configurations. So the objective of this research is to conduct a detailed analysis on the operating characteristics during the long-time combustion process. A better understanding of the combustion process will benefit the investigation of scramjet performance, including the self-ignition, stable combustion, fuel regression rate and trend of specific thrust. In this study, we built a vitiated air heater with combustion temperature in the 1200 ~ 2000 K, and designed different combustor configurations, in order to study the ignition characteristics at a high total temperature (1600 K). Meanwhile, the operating time of vitiated air heater was extended in order to investigate the characteristics of a long-time working scramjet combustor. Finally, combustor which uses a step as the flame holder has a higher filling factor (as shown in Figure 2) compared to the combustor which uses a cavity, but research of the combustor performance with step is still scarce, so we designed different combustors with cavity or step to study combustion characteristics.

2. Experiment apparatus and systems

By increasing the total enthalpy of the airflow, scramjet experimental system simulates the combustor inlet conditions under certain flight environments, and records the performance of scramjet. The experimental apparatus is shown schematically in Figure 3. It is composed of four major elements: the vitiated air heater, the gas and cold water supply system, the control and data acquisition system, and the experimental combustor.

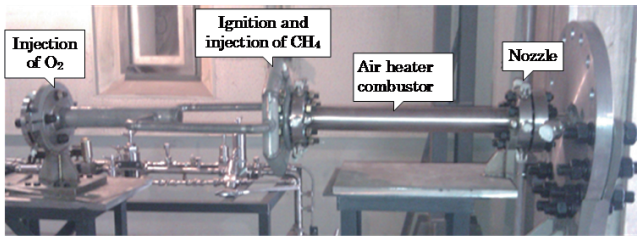


Figure 4 Vitiated air heater.

2.1 Vitiated air heater

Vitiated air heater is the core element of the scramjet experiment system, and it is used to increase the total enthalpy of the airflow by way of combustion of fuel. Oxygen is injected at the front of vitiated air heater in order to keep same oxygen mass fraction with air. And we require the airflow with high purity at the heater exit, to verify the self-ignition of combustor. So we choose methane as the vitiated air heater’s fuel, and the main design specifications are as follows:

- 1) Air mass flow rate (0.5~1) kg s⁻¹.
- 2) Airflow total temperature (1200~2000) K.
- 3) Airflow total pressure (2~4) MPa.
- 4) Combustion efficiency (> 0.95).

Vitiated air heater is divided into three parts: oxygen supplement section, combustion section and nozzle, as shown in Figure 4. Oxygen supplement section is used to supplement oxygen consumed by combustion of methane, and the nozzle to simulate different inlet conditions.

2.2 Gas and cold water supply system

Four kinds of gas are required in the experiment: air, oxygen, methane and nitrogen. Air is the main working medium for vitiated air heater, and methane is fuel to increase the total enthalpy of airflow. Oxygen is used to supplement the consumed oxygen in air by methane, and nitrogen is used as sweep gas and to regulate the flow. The working temperature of vitiated air heater is as high as 2000 K, in order to ensure its long-time working stability, we use the active water cooling.

2.3 Control and data acquisition system

We use SIMATIC WinCC of Siemens to increase the safety and reliability of control system, video camera to record the variation of the fuel port contours during burning, and data acquisition card to record the pressure data.

2.4 Combustor

A kind of solid-fuel scramjet combustors, as shown in Figure 5, consist of a cavity flame holder, a cylindrical combustor, and an expanding combustor. Cavity plays a role in stabilizing the flame and promoting mixing of fuel and airflow. As Mach number increasing, the total pressure loss caused by heating increases, so after the cavity there is a cylindrical combustor to reduce the airflow Mach number. Meanwhile, in order to improve engine performance, there is an expanding combustor after cylindrical combustor, which is used to maintain supersonic flow with no choking because of the addition

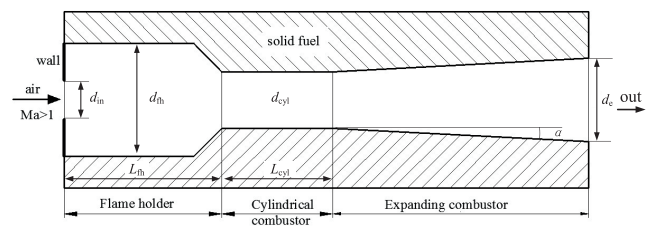


Figure 5 Configuration of the combustor.

Table 1 Summary of inlet conditions and working time.

Combustor number	p_0 [MPa]	T_0 [K]	Ma	m [g s ⁻¹]	t [s]
1	2.42	1580	1.6	536	20
2	2.38	1658	1.6	505	15
3	2.39	1591	1.6	531	15
4	2.44	1574	1.6	541	15
5	2.41	1593	1.6	534	5

of heat and mass.

3. Results and discussion

In this paper, we successfully conducted five experiments to simulate the flight conditions of Mach 6 and altitude 25 km. The appropriate combustor inlet conditions as show in Table 1, include total pressure, total temperature, Mach number, mass flow rate and working time.

PMMA materials are used in the combustor. Combustor 1 is designed according to the study results of Ben-Yakar^{4),5)}, which could successfully achieve self-ignition and stable combustion. And its working time is 20 s, much longer than the previous study. In order to investigate the influence of different expanding section expansion ratio on the combustion and internal ballistic, combustor 2 is designed, which has the same configuration with combustor 1 except a larger expansion ratio. Combustor 3 is designed with a step instead of cavity as the flame holder, which has a high filling factor (as shown in Figure 2) and has used in the solid-fuel ramjet, and combustor 4 has a deeper step than combustor 3. So according the study of combustor 1, 2 and 3, we can find a best structure for flame holding in the solid-fuel scramjet. Combustor 5 is designed with a large cavity and cylindrical section which is to investigate the influence of cavity size on the combustion. Meanwhile, there are 4 pressure sensors to test the wall pressure along the axis of combustor, numbered 1, 2, 3, 4, and their configurations are shown in Figure 6 ~ Figure 10. Then we put the geometry parameters of the five combustors in Table 2.

3.1 Characteristics of the long-time working combustor

The working times in Ben-Yakar and Cohen’s⁴⁾⁻⁶⁾ experiments are about 12s. In order to study the characteristics in a long-time working combustor, we design combustor 1 whose working time is 20 s.

Figure 11 shows the wall pressure traces of 4 sensors in combustor 1. During the test, operation starts with cold

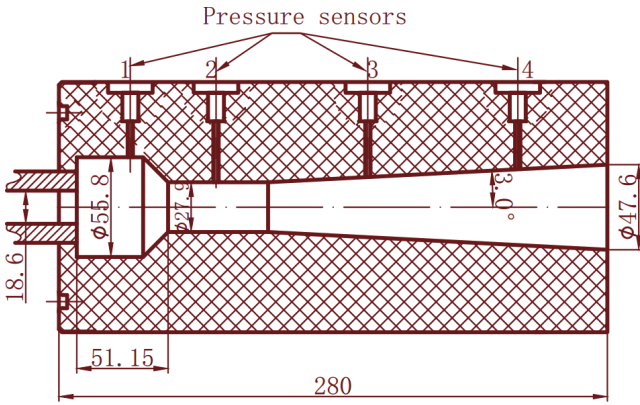


Figure 6 Configuration of combustor 1.

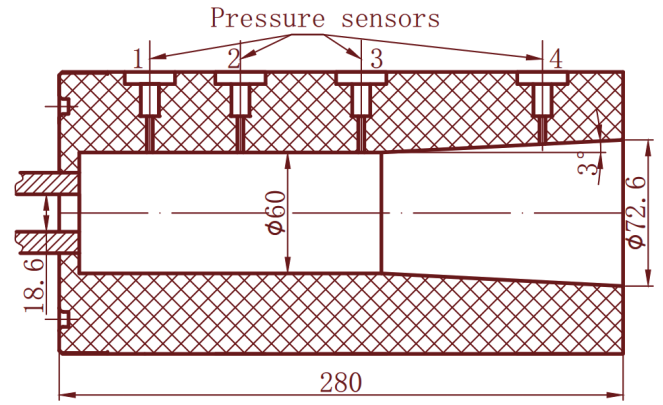


Figure 9 Configuration of combustor 4.

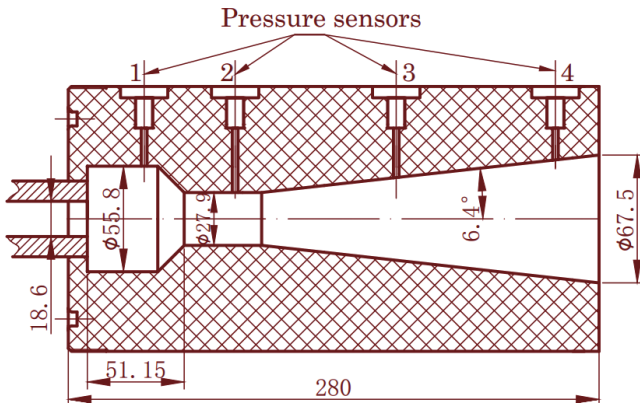


Figure 7 Configuration of combustor 2.

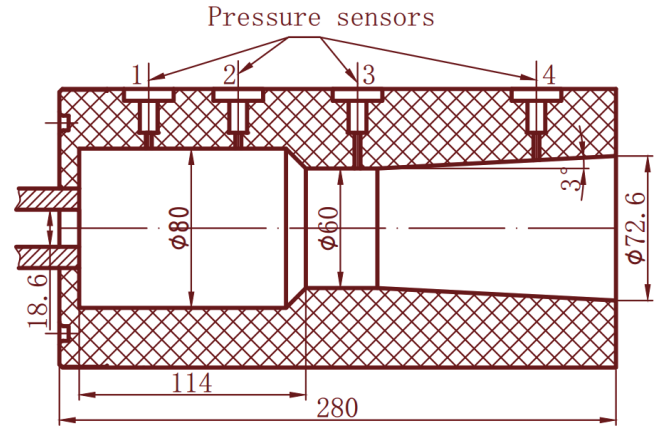


Figure 10 Configuration of combustor 5.

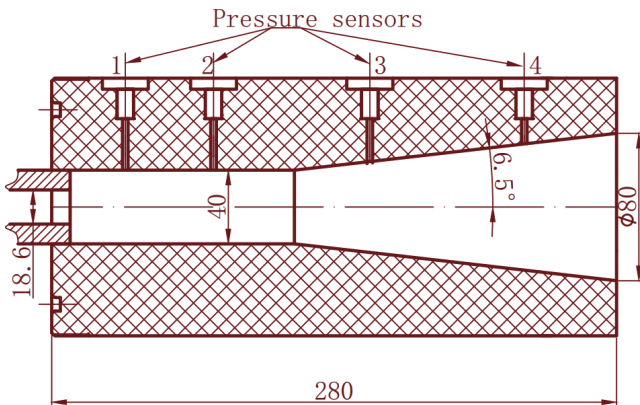


Figure 8 Configuration of combustor 3.

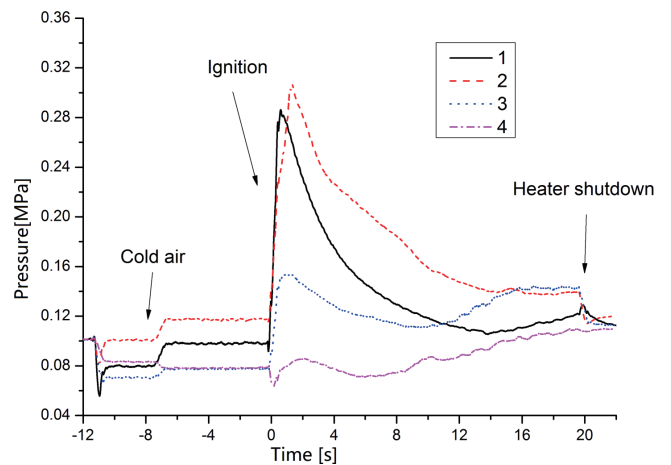


Figure 11 Wall pressure traces of combustor 1.

Table 2 Summary of combustors configuration.

Combustor number	Flameholder type	Step height [mm]	Cavity D_{fh} [mm]	Cavity L_{fh} [mm]	Cylindrical D_{cyl} [mm]	Expansion angle [°]
1	cavity	/	55.8	8.25	27.9	3
2	cavity	/	55.8	8.25	27.9	6.4
3	step	40	/	/	/	6.5
4	step	60	/	/	/	3
5	cavity	/	80	26.36	60	3

airflow through the combustor at -11 s, then adding oxygen at -8 s. And air heater starts to ignite with methane addition at 0 s. The maximum wall pressure of combustor 1 is about 0.3 MPa, much less than the inlet

total pressure (2.42 MPa), so there is no choking occurring. That is to say, the airflow in combustor is supersonic all the time.

After the air flow into the combustor, a bright flame

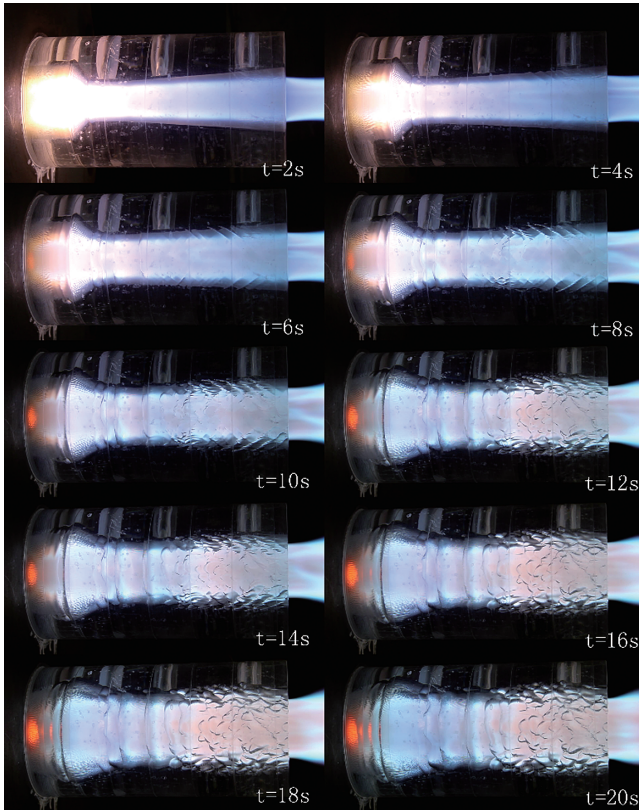


Figure 12 Sequence of video images of combustor 1.

appears in the cavity and cylindrical combustor resulting in a lot of light and heat, as shown in Figure 12. The cavity and cylindrical combustor are ignited, the total temperature increases. So the pressures of sensor 1, sensor 2 and sensor 3 increase rapidly. Combustor is able to self ignite. As combustor burning, its port contours are also starting to change. Cavity gets larger and deeper slowly, the diameters of cylindrical section and expanding section increase. So airflow expands gradually and the pressure of sensor 1-4 decrease gradually. But the cavity still exists. This is the necessary condition that combustor can work stably.

As time go on, the connecting portion of the cylindrical section and the expanding section disappears, and the cylindrical section and the expanding section become a “longer” expanding combustor. And then, the expansion ratio of expanding combustor decreases, expanding combustor gradually becomes a combustor with same diameter. So the pressure of sensor 3 and 4 increase gradually because of the addition of heat and mass. At the same time, the surfaces become more and more irregular, complex wave systems appear in expansion section which make the pressure of sensor 3 and 4 begin to fluctuate.

Figure 13 shows the fuel port contours during burning. We can see that the regression depth of various parts in combustor 1 at varying time. The regression depth at cavity gradually increases along the X axis, but at cylindrical section and expanding section decrease, and it gets a maximum depth at the connecting portion of the cavity and the cylindrical section. All of these conform the characteristics of combustor contours. Cavity gets larger and deeper like an inverted parabola, and angle of the

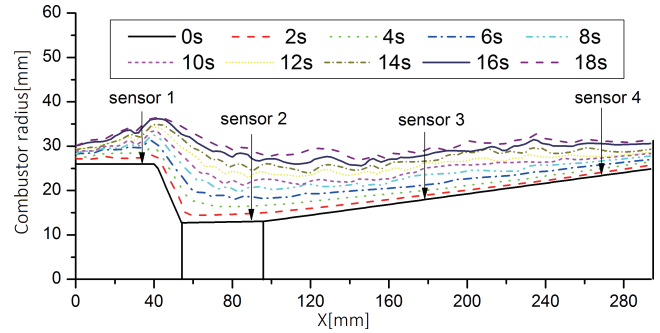


Figure 13 Variation of the fuel port contours during burning (Combustor 1).

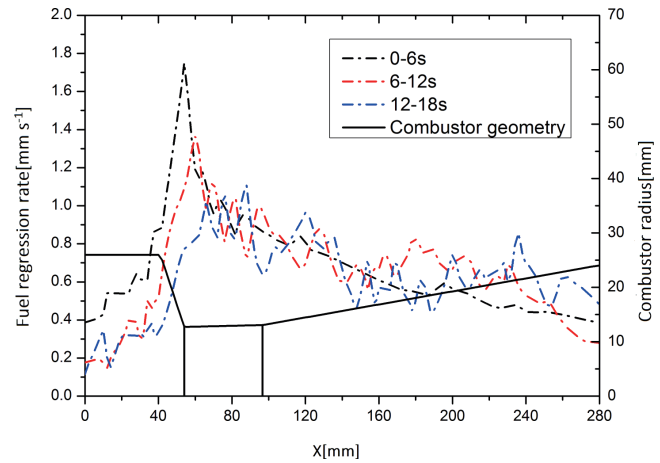


Figure 14 Axial variation of the time-average local regression rate (Combustor 1).

connecting portion between the cavity and cylindrical section decreases. Cylindrical section integrates with expanding section, and the expansion ratio decreases.

The measurement and prediction of regression rate are always the focus of scramjet research, which have a great effect on the airflow velocity, chemical reaction, mass and heat addition and flow field structure, as well as the overall performance of the engine. Compared with variation of the fuel port contours during combustion, we calculate the axial variation of the time-average local regression rate, as shown in Figure 14.

From Figure 14, we can see that the time-average local regression rate at the cavity increases gradually along the x axis, and it get a maximum rate at the connecting portion between the cavity and cylindrical section. The maximum rate decreases with time. At the cylindrical section and expanding section, the time-average local regression rate decrease gradually. Meanwhile, the time-average local regression rate fluctuates substantially after the 6s, which was due to shock effects. This corresponds well to the Figure 12, that the surfaces of expanding combustor become more and more uneven with time.

The conclusions are consistent with Ben-Yakar and Gany^{(4), (5)} experimental results. From the numerical point of view (Figure 15 and Table 3), the average regression rate is larger than the rate of Ben-Yakar and Cohen's^{(4) - (6)} results. According to the over regression rate by Cohen⁽⁶⁾, as Equation (1) shows, the inlet total temperature and mass flow rate have larger effects on average regression

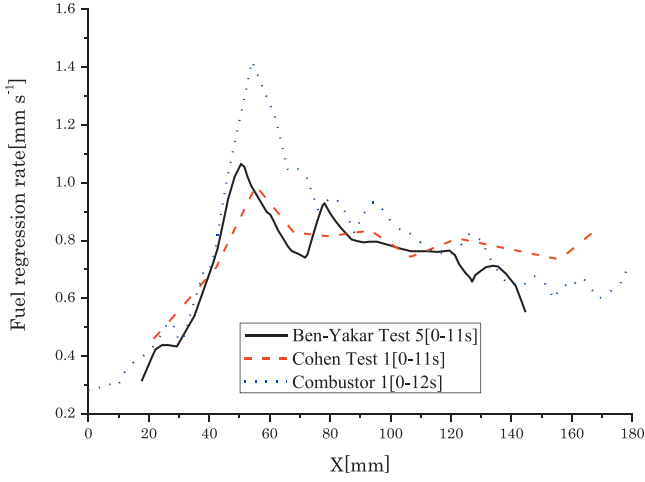


Figure 15 Axial variation of the time-average local regression rate.

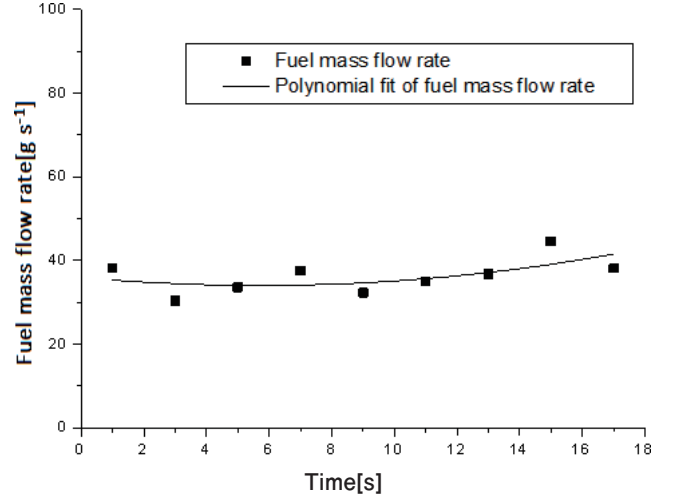


Figure 16 Overall fuel mass flow rate of combustor 1.

Table 3 The average regression rate.

	No.	p_0 [MPa]	T_0 [K]	m [g s ⁻¹]	r [mm s ⁻¹]
Ours	Combustor 1	2.42	1580	536	1.2
Cohen	Test 1	3.73	1276	302	0.8
Ben-Yakar	Test 5	1.69	1156	183.8	0.7

rate than total pressure. This is why that our result is larger than theirs.

$$r \propto m_{\text{Air}}^{0.85} \cdot T_{0,\infty} \cdot p_{0,\infty}^{0.2} \quad (1)$$

Then, we calculate overall fuel mass flow rate according to Equation (1) and Figure 13.

$$m_{\text{fuel}} = \int_0^L \rho \pi r dx \quad (2)$$

Figure 16 shows the overall fuel mass flow rate of combustor 1 at varying time. Before 8s, overall fuel mass flow rate remains constant substantially, which is consistent with the Ben-Yakar^(4),5) conclusion. But due to the higher inlet total temperature, the value of overall fuel mass flow rate in our experiment is larger. Meanwhile, overall fuel mass flow rate increases a little after 8s. That because a lot of shock appears in flow field, which have an effect on the chemical reaction and make the time-average local regression rate fluctuate substantially. The surfaces of expanding combustor become more and more uneven and non-axisymmetric. Meanwhile, the uneven and non-axisymmetric surfaces also make the calculations different. It needs further research.

So far, the test cannot measure thrust. In order to study the overall performance of combustor, we use Wang's quasi-one-dimensional numerical method^(16),17) to calculate the thrust of combustor 2 and the thrust variation at varying time, which has been proved to have a high accuracy comparing to experiments.

We distinguish between thrust into the ground thrust and thrust under flight environment. Ground thrust is measured by experiment on ground. Thrust under flight environment is the thrust generated by the combustion chamber airflow reaches an ideal expansion after passing through the nozzle, at this time, the nozzle outlet airflow pressure is equal to the flight environment pressure.

Ground thrust is defined as follows:

$$F_{\text{ground}} = m_e \cdot v_{\text{ground}} + (p_{\text{ground}} - p_a) \cdot A_e \quad (3)$$

The static pressure at ground is higher than that at the flight environment, the gas at the outlet of the combustor cannot expand adequately. So at the same inlet conditions and same combustor, thrust under flight environment is larger than ground thrust. Supposing that the airflow reaches an ideal expansion state in the nozzle, the thrust under flight environment is defined as follows:

$$F_{\text{flight}} = m_e \cdot v_{\text{ideal}} - m_{\text{air}} \cdot v_{\text{flight}} \quad (4)$$

The ideal exit velocity

$$v_{\text{ideal}} = \sqrt{\frac{2k}{k-1} RT_0 \left[1 - \left(\frac{p_c}{p_{\text{in}}} \right)^{\frac{k-1}{k}} \right]} \quad (5)$$

The specific thrust is defined as thrust per unit mass flow rate of air:

$$F_{\text{sp}} = \frac{F_{\text{flight}}}{m_{\text{air}}} \quad (6)$$

Figure 17 shows the specific thrust of combustor 2 at varying time. When the combustion efficiency is about 70%⁽⁷⁾, the specific thrust is at a level of about 700 ~ 900 N s kg⁻¹, which is larger than the result in the Li-he Wang's research^(16),17) (600~800 N s kg⁻¹). That is because the configuration of combustor and the inlet conditions are different from our experiment, that air mass flow rate is 1 kg s⁻¹, and inlet total temperature is 1500K. The rate of change of specific thrust decreases gradually with time, and the specific impulse is shown in Figure 18, which also decreases gradually with time.

In the experiment, we find that mass flow rate is relatively stable. So we can conclude that the decrease of

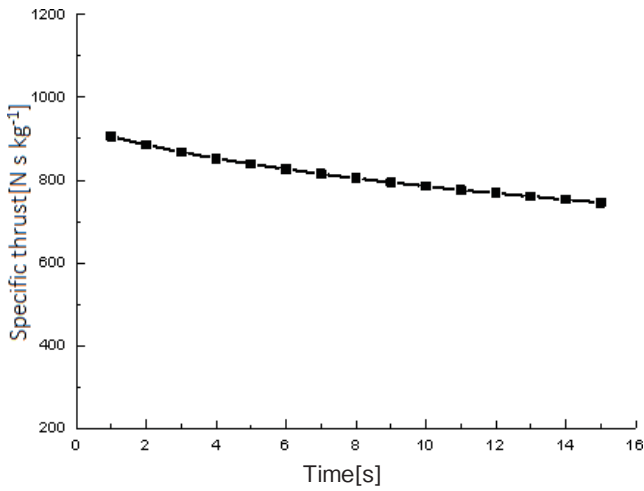


Figure 17 Specific thrust of combustor 2 at varying time.

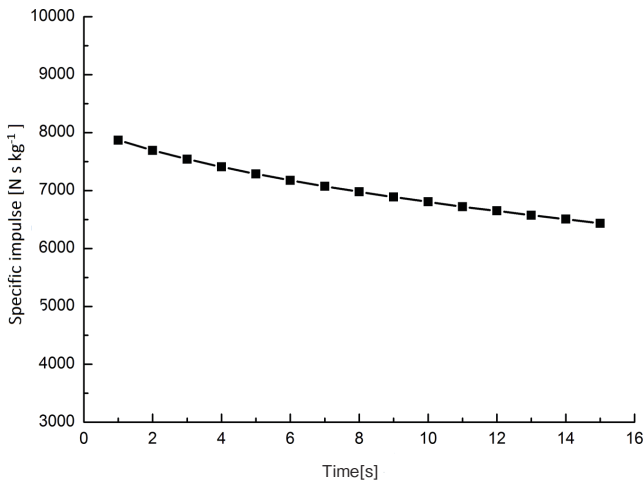


Figure 18 Specific impulse of combustor 2 at varying time.

specific thrust is due to the decrease of exit velocity, according to Equation (3) and Equation (4). From Equation (5), we can see that the exit velocity affected by the total temperature and the total pressure of the combustor: The smaller the total temperature or the total pressure, the smaller the ideal exit velocity. Since the combustion efficiency is relatively stable⁽⁷⁾, so the total temperature is stable. Then we can make a conclusion that the decrease of specific thrust is due to the decrease of total pressure, and this is consistent with Pei^(14,15) conclusion that the total pressure loss is increasing over time.

So we can conclude that the fuel regression rate decreases gradually with time in the course of a long-time working combustor, but the fuel mass flow rate remains constant substantially. The cylindrical section disappears and the entire combustor behind the cavity become a larger straight cylindrical combustor. The burning surfaces become uneven. Thrust and specific thrust and specific impulse decreases gradually with time, because of the decrease of total pressure.

3.2 Expansion ratio, cavity and step

3.2.1 Expansion ratio

In order to investigate the influence of different expansion ratio (the ratio of outlet area and inlet area of expanding section) on the internal ballistics, combustor 2

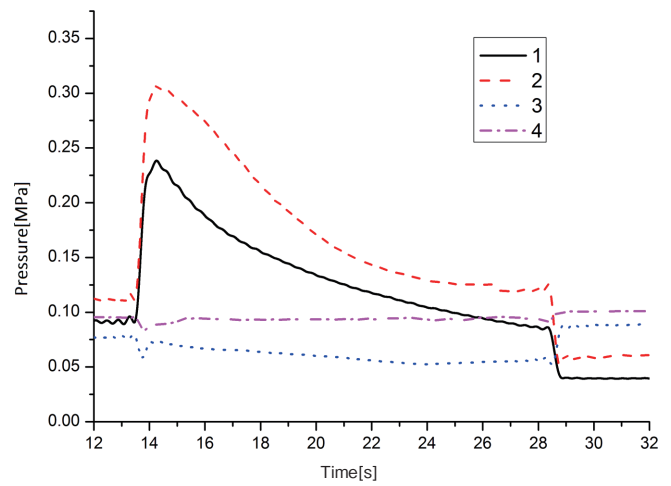


Figure 19 Wall pressure traces of combustor 2.

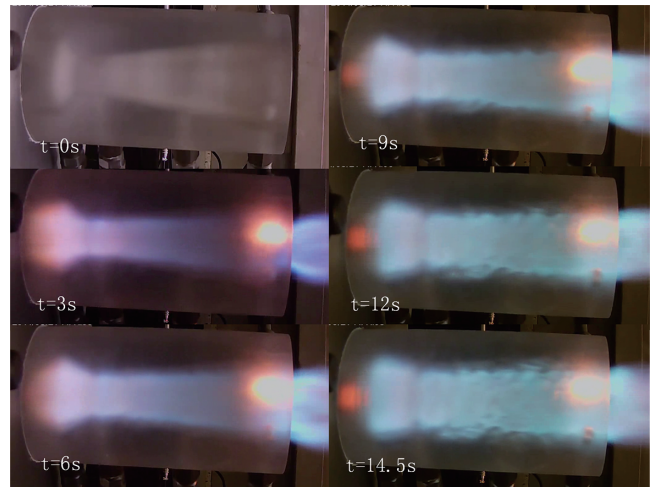


Figure 20 Sequence of video images of combustor 2.

is designed which has the same configuration with combustor 1 except a larger expansion ratio. The interior ballistics of combustor 2 is shown in Figure 19 and video images of combustor 2 are shown in Figure 20.

As Figure 19 and Figure 20 show, after the air flow into the combustor, a bright flame appears in the cavity and cylindrical combustor. The cavity and cylindrical combustor are ignited, the total temperature increases. So the pressures of sensor 1 and sensor 2 increase rapidly, combustor is able to self-ignite. Then, the diameters of the cavity and the cylindrical section increase, airflow expands gradually, so the pressures of sensor 1 and sensor 2 decrease gradually.

From Figure 20 we can see that the expansion ratio of combustor 2 is gradually reduced, but due to the increase of the port area, the airflow is stably expanded in the expansion section, so the pressure of sensor 3 and sensor 4 are stable, and both below the atmospheric pressure. According to the expansion theory, the pressure of sensor 4 should be lower than sensor 3. However, we see the opposite conclusion from Figure 19. This is because the expansion ratio of expanding section is too large, the airflow expands excessively, resulting in the formation of the oblique shock and the boundary layer separation due to the back pressure gradient. The sensor 4 is behind the separation point, so its pressure will rise and be

approximately equal to the ambient pressure, which is obviously not conducive to produce thrust.

Comparing Figure 11 and Figure 19, the interior ballistics of combustor 1 and combustor 2 are very similar to each other. The cavity and the cylindrical section pressure will quickly rise and then fall slowly, the pressure in the expanding section is stable relatively. However, the difference is that the expanding ratio of combustor 1 is smaller than that of combustor 2, then airflow can only slowly expand, so that pressure of sensor 3 is larger than sensor 4 in combustor 1. As we all know, expanding section has played a role in the expansion of accelerating airflow, when in flight environment, the ambient pressure is much smaller than that on ground, so larger expansion ratio will be contributed to airflow expanding and thrust. But expansion ratio does not have effect on the internal ballistic of cavity and cylindrical combustor.

3.2.2 Cavity and step

In order to find a best structure for flame holding in the solid-fuel scramjet, combustor 3 and 4 are designed with a step instead of cavity as the flame holder, which has used in the solid-fuel ramjet. As shown in Figure 21, the interior ballistics of combustor with a step structure show completely different characteristics. The video images of combustor 3 are shown in Figure 22.

From Figure 21, the pressure of sensor 1 increases rapidly after combustor ignition, and decreases gradually with fluctuations after maintaining a period-time constant. The pressure of sensor 2 increases slightly at first, and appears a sudden rise in the medium-term. Then it decreases with fluctuations. The values of sensor 1 and 2 are much lower than the previous tests, this is because that the diameter of cylindrical combustor 3 is much larger than combustor 1 and 2, then the airflow expands more fully in combustor 3. Sensor 1 is at the attachment point of airflow and combustor. Due to the erosion of airflow and combustion, the pressure of sensor 1 does not decrease rapidly. Since the combustion before 4s is very unstable, the pressure of sensor 1 will be unstable fluctuations.

From Figure 22, the combustor with step cannot maintain a stable flame at first in the combustion process. The flame is blown to the expanding section and stabilized after a shock wave which is formed in the expanding section. Until a shallow "cavity" is formed at the front of the combustor, the cylindrical section begins to appear bright flame. As Figure 22 shows, cavity is washed out by airflow at $t = 4.9$ s, this corresponds well to Figure 21 that the pressure of sensor 1 decreases significantly at the same time. After the formation of the cavity, the point of sensor 1 is in a stable low-speed zone, which result the increase of pressure. As the combustion progresses, the port area of combustor increases, the airflow expansion increases, and the pressure begin to slowly decrease, which is the same with other combustors. On the other hand, sensor 2 is between the cavity which formed at 4.9s and the expanding section, where is equivalent to a converging section. So, the airflow is compressed, and

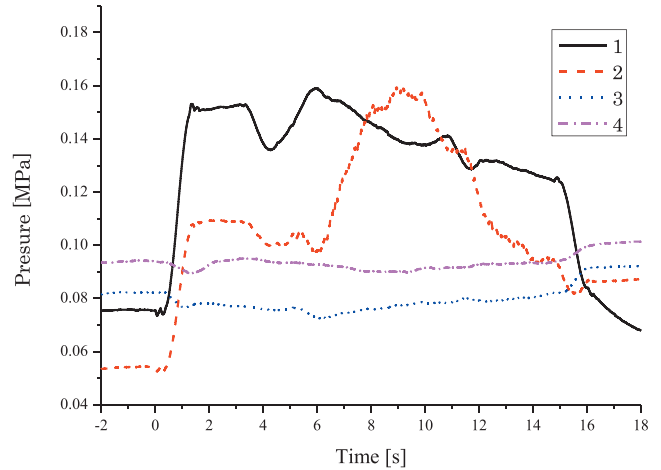


Figure 21 Wall pressure traces of combustor 3.

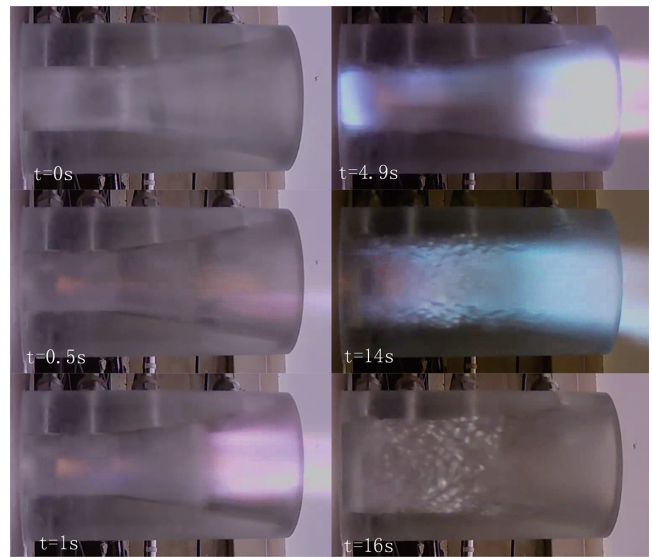


Figure 22 Sequence of video images of combustor 3.

pressure increases, ultimately reaches a maximum value, which is larger than the pressure of sensor 1. This is consistent with combustor 1 and combustor 2. With the increase of port area, compression at the point of sensor 2 slowly weakening, and the pressure gradually decreases.

From the analysis above, we can conclude that the shallow steps do not play a role in stabilizing the flame until a small cavity is formed at the front of combustor. On the other hand, could a deeper step play a role in stabilizing the flame? Figure 24 shows the video images of combustor 4, which has a deeper step than combustor 3. We can see from Figure 24 that a deeper step still cannot maintain a steady flame, either. The combustion process of combustor 4 is similar to the combustor 3. At first, combustion occurs in the expanding section. Until a small cavity appears at the front of combustor, there is a bright flame throughout entire combustor. However, the cavity appears at 4.9 s in combustor 3 and at 7.7 s in combustor 4. So the height of the steps have an impact on the time of cavity appears, the deeper the steps, the later time of the cavity appears. That is to say, combustor with a shallow step is able to stabilize combustion earlier than that with a deep step.

Comparing Figure 21 and Figure 23, we can see that the

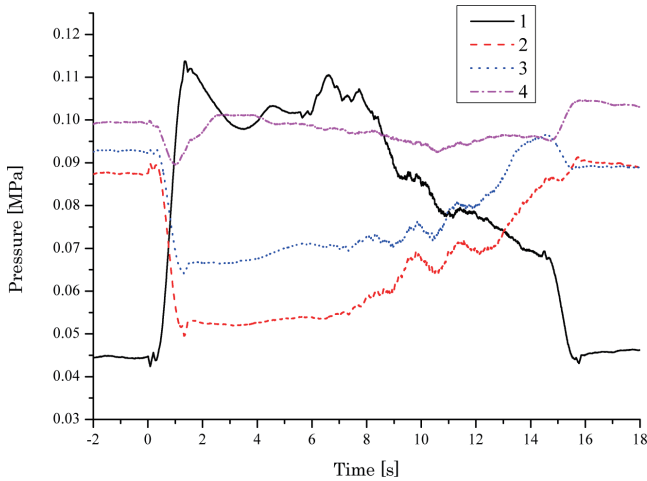


Figure 23 Wall pressure traces of combustor 4.

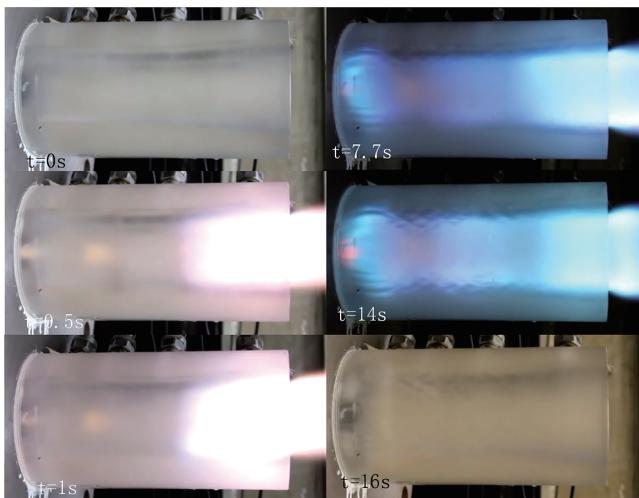


Figure 24 Sequence of video images of combustor 4.

pressures of sensor 1 and 4 in combustor 3 are similar to the pressures in combustor 4. Pressure of sensor 1 increases first and then decreases, and pressure of sensor 4 at the expanding section is affected by the ambient pressure and changes little for the same reason of combustor 1. The pressures of sensor 2 and 3 in combustor 4 are significantly lower than the pressure in the combustor 3, and have a slow upward trend. That is because the port area of combustor 4 is larger, airflow expands more fully. And then, cavity appears, flame is stabilized, total temperature and static pressure increase.

But continuing to increase the height of the step, it will increase total pressure loss due to sudden expansion of airflow^{(10),(14),(15)}, and reduce the filling factor of combustor. So step is not suitable for flame holding in the solid fuel scramjet.

3.3 Ignition characteristics at high total temperatures

Ben-Yaker used PMMA as fuel conducted a series of combustor ignition tests, and they found the facts: the small black squares indicate that combustion cannot be sustained, the small white squares indicate that combustion can be sustained. Then Ben-Yaker summarized the flameholding limits figure based on their test results, as shown in Figure 25, for a given $(D_{th}/D_{cyl})^2$, if

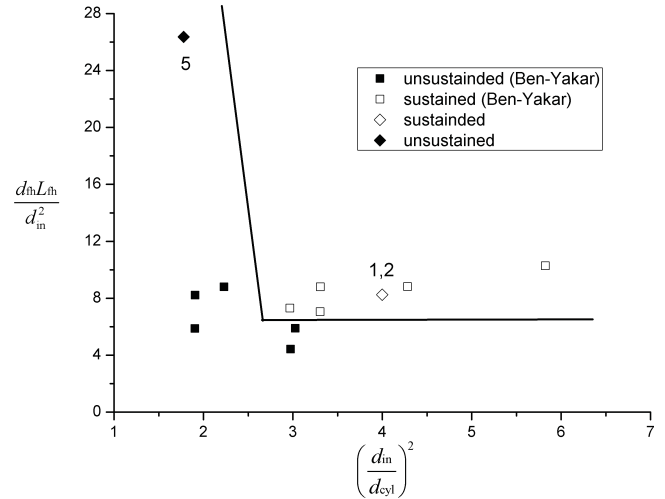


Figure 25 Flameholding limits in the solid fuel scramjet combustor.

$(D_{th} L_{th})/D_{in}^2$ is above the solid line, the combustion chamber is able to self-igniting and maintains flame stability; if $(D_{th} L_{th})/D_{in}^2$ is lower than the solid line, the combustion chamber cannot maintain flame stability. In our experiments, for the cavity of the combustor 5, after calculation, it was found that $(D_{th} L_{th})/D_{in}^2$ is lower than the solid line, expressed as diamond lattice in Figure 25. This means that according to Ben-Yaker's conclusion, combustor 5 should not be able to sustain combustion. However, in our test, combustor 5 was ignited. The main difference between our test conditions and Ben-Yaker, Cohen is the inlet total temperature (the inlet total temperatures of their tests are from 1100 K to 1400 K, less than our test's 1600 K). At the same time, Ben-Yaker found that combustor only with a step cannot ignite, but our test shows that combustor 3 and 4 (only with a step) can ignite successfully. Above all, it can be concluded that self-ignition performance is not only related to depth and length of the cavity, but also related to the inlet total temperature; and when the inlet total temperature is high enough, even with step, self-ignition can also succeed.

For the combustors with cavity (combustor 1, 2, 5), do the size of the cavity have any effect on the ignition performance? We can see from Figure 26 that the flame has successfully filled the entire combustor 1 in 1/24 s, but there is still not completely filled in combustor 5. The reason is that the cavity and cylindrical section diameter of combustor 5 is too large, the airflow in the combustor 5 will continue to expand, accelerate, and it will consume more energy for the ignition. So it can be concluded that the larger the cavity, the longer time the ignition of combustor.

Comparing the pressure traces of combustor 1 and 5, as shown in Figure 11 and Figure 27, we find that at a high inlet temperature, even if the combustor with a large cavity (combustor 5) has been successful self-ignition. The pressures of cavity (sensor 1, sensor 2) and cylindrical section (sensor 3) increase rapidly, but they are still less than ambient pressure. This is not contributive to fuel mixing, combustion and produce thrust. Meanwhile, if the cavity is too large, it will reduce the fuel filling factor and

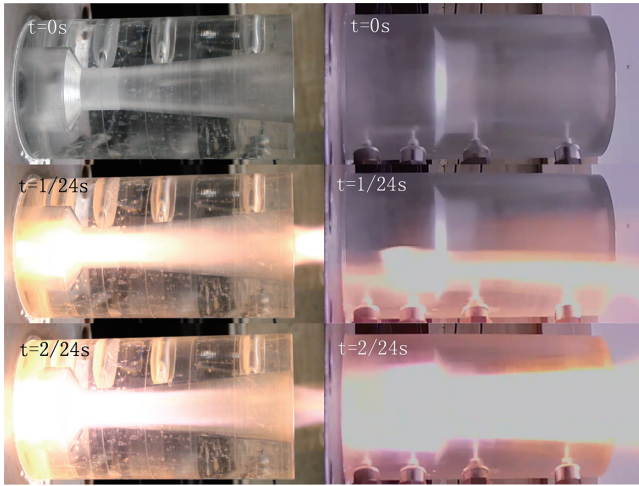


Figure 26 Ignition images of combustor 1 and 5.

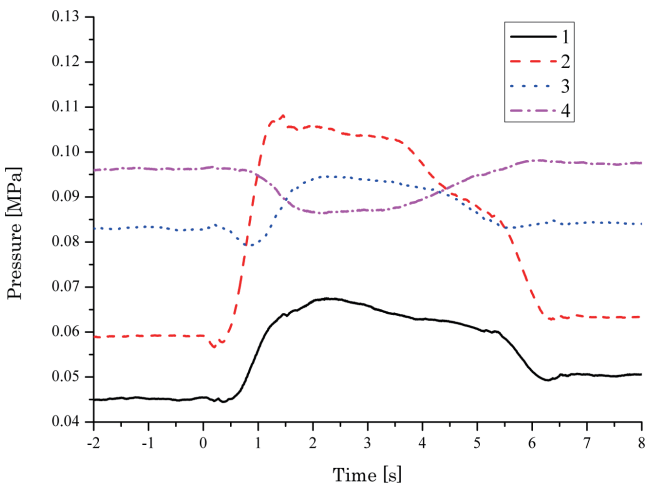


Figure 27 Wall pressure traces of combustor 5.

cause the engine's endurance to decline.

4. Conclusions

A series of PMMA solid fuel combustors have been analyzed, designed, and successfully demonstrated experimentally, simulating the flight conditions of Mach 6 and altitude 25 km. The appropriate combustor inlet conditions of total air temperature and pressure are 1600 K and 2.4 MPa, respectively. A video camera is adopted to record the combustion process and wall pressures of combustors are measured by 4 pressure sensors. We can get the following conclusions:

In a long-time working scramjet combustor, the fuel mass flow rate is able to sustain substantially constant, but specific thrust and specific impulse decrease gradually with time. The regression rate gets a maximum rate at connecting portion of the cavity and cylindrical section, but it decreases with time. During the combustion process, cavity gets larger and deeper slowly. The entire combustor behind the cavity gradually becomes straight and appears uneven pits, which become more obvious

with time. So there will be little fuel left after combustion.

And steps cannot play a stabilizing role in the solid fuel scramjet until a cavity appears, and the deeper the steps, the later time of the cavity appears.

Self-ignition performance is not only related to depth and length of the cavity, but also related to the inlet total temperature. When the inlet total temperature is high enough, even with step, self-ignition can also succeed. And the larger the cavity, the longer the ignition time needs.

Acknowledgments

This study was supported by the National Natural Science Foundation of China (Grant No. 51276020).

References

- 1) M. A. Witt, The NPS Institutional Archive, Monterey, CA (1989).
- 2) W. J. Angus, The NPS Institutional Archive, Monterey, CA (1991).
- 3) W. J. Angus, M. A. Witt, and D. Laredo, *La Recherche Aeronautique*, 6, 1–8 (1993).
- 4) A. Ben-Yakar, B. Natan, and A. Gany, *J. Propul. Power*, 4, 447–455 (1998).
- 5) A. Ben-Yakar and A. Gany, Proc. 30th AIAA/ASME/SAE/ASEE Joint Propul. Conf., 1994–2815, AIAA, Indianapolis (1994).
- 6) A. Cohen-Zur and B. Natan, *J. Propul. Power*, 6, 880–889 (1998).
- 7) S. Saraf and A. Gany, Proc. 18th International Symposium on Air Breathing Engines, 2007–1176, ISABE (2007).
- 8) D. Simone and C. Bruno, *J. Propul. Power*, 25, 875–884 (2009).
- 9) D. Simone and C. Bruno, Proc. 47th AIAA Aerospace Sciences Meeting Including The New Horizons Forum and Aerospace Exposition, 2009–2813, AIAA, Orlando (2009).
- 10) H. Tao and Z. Wei, Proc. 49th AIAA/ASME/SAE/ASEE Joint Propul. Conf., 2013–3974, AIAA, San Jose (2013).
- 11) H. Chi, Z. Wei, B. Li, and L. Wang, Proc. 50th AIAA/ASME/SAE/ASEE Joint Propul. Conf., 2014–3451, AIAA, Cleveland (2014).
- 12) C. Liu, Z. Wei, H. Chi, and N. Wang, Proc. 50th AIAA/ASME/SAE/ASEE Joint Propul. Conf., 2014–3452, AIAA, Cleveland (2014).
- 13) B. Li, Z. Wei, and H. Chi, Proc. 49th AIAA/ASME/SAE/ASEE Joint Propul. Conf., 2013–3695, AIAA, San Jose (2013).
- 14) X. Pei, Z. Wu, Z. Wei, N. Wang, and J. Liu, *J. Propul. Power*, 5, 1041–1051 (2013).
- 15) X. Pei, Z. Wu, Z. Wei, N. Wang, and J. Liu, Proc. 48th AIAA/ASME/SAE/ASEE Joint Propul. Conf., 2012–3830, AIAA, Atlanta (2012).
- 16) L. Wang, H. Chi, C. Liu, H. Tao, and Q. Wang, Proc. 50th AIAA/ASME/SAE/ASEE Joint Propul. Conf., 2014–3453, AIAA, Cleveland (2014).
- 17) L. Wang, Z. Wu, H. Chi, C. Liu, H. Tao, and Q. Wang, *J. Propul. Power*, 2, 685–693 (2015).